PCCP

Accepted Manuscript

ROYAL SOCIETY OF CHEMISTRY

www.rsc.org/pccp

Journal Name

RSCPublishing

ARTICLE

Tailoring the Properties of Quadruplex Nucleobases for Biological and Nanomaterials Applications†

Jan Novotný,[a,b] Yevgen P. Yurenko,[a] Petr Kulhánek,[a,b] Radek Marek [a,b,c*]

Cite this: DOI: 10.1039/x0xx00000x

Received ooth January 2012,
Accepted ooth January 2012

DOI: 10.1039/x0xx00000x

www.rsc.org/

Guanine DNA quadruplexes are interesting and important biological objects because they represent potential targets for regulatory drugs. Their use as building blocks for biomaterial applications is also being investigated. This contribution reports the *in silico* design of artificial building blocks derived from xanthine. Methods of quantum chemistry were used to evaluate the properties of xanthine structures relative to those containing guanine, the natural reference used. Tailoring the xanthine core showed that the base stacking and the ion coordination were significantly enhanced in the designed systems, while the ion-transport properties were not affected. Our study suggests that the 9-deaza-8-haloxanthine bases (where the halogen is fluorine or chlorine) is highly promising candidate for the development of artificial quadruplexes and quadruplex-active ligands.

Introduction

The G-quadruplexes, guanine-rich repetitive oligonucleotide sequences with a tetrahelical structure are interesting biologically because of their crucial role in the cellular genome.[1] G-quadruplexes have also been recognized as suitable motifs for various applications in nanoscience.[2] In addition, several structures built from nucleobases other than naturally occurring guanine, but manifesting the same key non-covalent interactions as those seen in G-quadruplexes have been reported. Most notably xanthine assemblies with supramolecular structures similar to those of guanine have been characterized experimentally and theoretically.[3–7] In this work, we investigate the key interactions in systems composed of xanthine and its derivatives to gain deeper insight into the interactions that govern the quadruplex structural and dynamic properties.[8] Their potential applications provide further motivation for screening and developing these systems. These structures might serve as binding domains of smart ligands that adhere specifically to the external faces of quadruplexes in cellular DNA.[9] The ligands we describe may enable the *in vivo* detection/visualization[10] or functional modulation of adjacent elements of the genome.[11,12] Materials science and biotechnology are other interesting areas where these compounds might be employed, e.g., as the building units of nanowires and biosensors.[13] They might also be used as ion-transport channels[14] and as ion-induced switches.[15]

The ideal prototype of a nucleobase should fulfil several fundamental requirements derived from the nature of the dominant binding forces in the quadruplex architecture: i) it should form a planar cyclic system containing stable hydrogen bonds (HBs) between the individual base units of the tetrad, ii) it should form helical stacks of tetrads (S) connected in oligonucleotide sequences by relaxed backbone, and iii) it should accommodate a cation (M^+) in the central pore of the system (for a general arrangement showing two stacked tetrads with one cation, see Figure 1).[16]

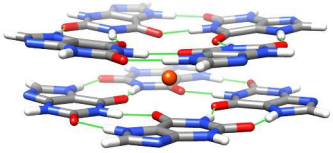

Figure 1. General arrangement of two stacked xanthine tetrads accommodating a monovalent cation in the inter-plane region. Hydrogen bonds are depicted using fine green lines.

This paper demonstrates the rational design of artificial nucleobases with desirable characteristics such as increased stability or ion-transport properties. We present a strategy for evaluating the potential ability of xanthine derivatives to adopt quadruhelical structures analogous to that of the guanine-based archetype. Particularly investigated are those systems derived from xanthine wherein the N3 atom (in contrast to the N9 atom in guanine) is accessible for a glycoside bond in an oligonucleotide or ligand application. For reference purposes, we employ systems composed of guanine or xanthine, that have been characterized experimentally.[3,17,18]

Single tetrad - B_4, two-stacked tetrads - $(B_4)_2$, and three-stacked tetrads - $(B_4)_3$ systems (without a sugar-phosphate

backbone) coordinating the cations Na^+ or K^+ are studied at various levels of complexity using density functional theory (DFT). Finally the stability of a four-stranded parallel quadruplex that contains both the most promising nucleobase candidate and a sugar-phosphate backbone is investigated by means of molecular dynamics (MD) simulations.

COMPUTATIONAL DETAILS

The stability of the system was evaluated by using the energy of formation. The formation energy was calculated using the Turbomole v6.3 package[19] with BLYP functional[20,21] and the def2-TZVPP basis set[22] and with a dispersion energy correction (D3) employing Grimme's scheme.[23] The calculation of the coulomb integrals was accelerated by using the Resolution of Identity (RI) approximation.[24,25] The polar contribution to the energy of solvation was included by using the COSMO solvent model[26] with the default atomic radii. The dielectric constant was set to 78.4 and the radius of the solvent probe to 1.93 Å in order to simulate the characteristic of an aqueous environment on the formation energy.[27,28] No counterpoise correction was applied to DFT-D3 formation energies because the small BSSE effects were shown to be absorbed by the dispersion potential.[29,30] The formation energies were calculated by using the formulas specified in the captions of the corresponding figures. If not stated otherwise, all geometries were fully optimized at the level of theory used to calculate the formation energies. Cartesian coordinates of the selected optimized models are available in Supporting Information.

To calculate the energy barrier to ion-transport through $(B_4)_3$ system, we prepared models optimized with constrained planarity. Subsequently, for each position of the ion, the Cartesian coordinates of the atoms of both of the outer tetrads were constrained and only the atoms of the central tetrad were allowed to relax (in contrast to a previous study, in which all of the tetrads were fixed[31]). For technical details, see Supporting Information.

Molecular dynamics simulations were carried out using the *pmemd* program of the AMBER 11 package.[32] The production simulations were performed at a constant temperature of 298 K and a constant pressure of 1 bar, using a 2 fs integration time step. Bonds involving hydrogen atoms were constrained. The simulated quadruplex was described by the ff99bsc0 force field.[33,34] The RESP charges of the modified nucleoside were derived using a procedure described in our previous work.[5] All simulations were carried out using the explicit water solvent described by the TIP3P model.[35] Counter ions were described by the parameterization of Joung, *et al.*[36] Further details of the MD simulations can be found in Supporting Information.

RESULTS AND DISCUSSION

Building blocks

The chemical structures of the xanthine derivatives investigated in this paper are shown in Figure 2. Their binding abilities were first qualitatively assessed by using partial atomic charges derived from the electrostatic potential by employing the Merz-Kollman scheme[37] (Figure 2, Table S2 in Supporting Information). We focused mainly on the O6 atom because we expected that the strength of the inner hydrogen bonds and the cation binding should be strongly influenced by the electron density at this atom.

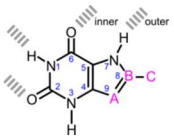

	X	MX	FX	daX	FdaX	CldaX	AdaX
A	N	N	N	CH	CH	CH	CH
B-C	C-H	C-CH_3	C-F	C-H	C-F	C-Cl	N
O6	-0.620	-0.639	-0.622	-0.640	-0.644	-0.626	-0.604

Figure 2. Structures and abbreviations for some modified xanthines (X, MX, FX, daX, FdaX, CldaX, and AdaX). The donor and acceptor sites for the inner and outer hydrogen bonds are highlighted. The values of the ESP atomic charge at the O6 atom are presented on the last line.

The values of the ESP atomic charge at the O6 atom were lower than that of the reference xanthine system for all of the derivatives except AdaX. This change is most noticeable for 9-deazaxanthine (daX, Δq = -0.020) and its fluorinated derivative (FdaX, Δq = -0.024). However, it should be noted that the accumulation of negative charge on O6 could generate repulsive forces between the oxygen atoms in the tetrads and the higher-order structures that would hinder aggregation in the absence of a cation. Moreover, these simple qualitative criteria neglect the effects of polarization and the cooperativity of hydrogen bonds within the quartets in addition to all of the other interactions within the higher-order assemblies.

The above-mentioned charge analysis indicates that the derivatives daX and FdaX are best suited to act as building blocks, but it is difficult to evaluate the suitability of the remaining derivatives by using such a simple assessment. We therefore investigated the stabilities of B_4, $(B_4)_2$, and $(B_4)_3$ assemblies in the presence or absence of a monovalent cation (Na^+ or K^+) by analyzing the formation energies.

Formation of a single tetrad – $B_4 \cdot M^+$

The formation of a single tetrad (B_4) and its coordination with an ion (M^+) as expressed in terms of energy is shown in Figure 3. The formation energy of this first step serves as a measure of the strength of the base pairing in tetrads. The contribution of base pairing to the stability of the system is enhanced (as compared to xanthine, the natural reference) by incorporating a halogen atom at position 8 (in FX, FdaX, and CldaX), probably due to increased polarization of the N7-H7 bond. Surprisingly, the attachment of electron-donating methyl group at position 8 (MX) had a similar stabilizing effect, which can be rationalized by the hyperconjugation and/or redistribution of the electron density at the carbonyl oxygen atoms. The negligible difference in the formation energy between the tetrads composed of AdaX and X (the reference system) correlates well with the previously demonstrated atomic charges.

One of the crucial steps in the formation of guanine-based quadruplexes is the chelation of a monovalent cation between the oxygen atoms.[38] This process was found to be almost 5 kcal mol^{-1} less efficient for tetrads composed of xanthine than for

those containing guanine. The incorporation of a halogen atom attached to position 8 (FX) does not improve the coordination properties. However, replacing N9 with CH to yield the 9-deazaderivative (daX) enhances the ion binding by 2 kcal mol^{-1}.

Combining the substituent effects on the energy of base pairing and ion coordination suggests that the derivatives FdaX and CldaX are the most promising candidates for the design of artificial quadruplex-binding ligands or quadruplex systems with increased stability.

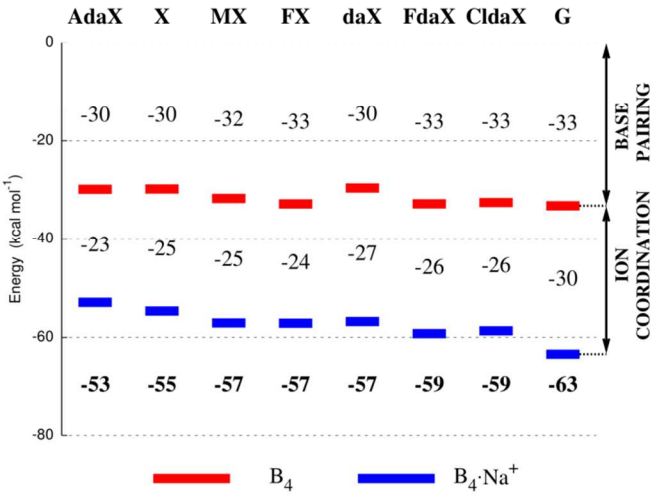

Figure 3. Contributions to the formation energy (ΔE) of the $B_4{\cdot}Na^+$ system in water. The total values of the formation energy are marked in bold. The other two values represent the individual contributions of the base pairing, calculated as $\Delta E = E[B_4] - 4 \times E[B]$, and the ion coordination, calculated as $\Delta E = E[B_4 \cdot Na^+] - \{E[B_4] + E[Na^+]\}$.

Formation of two stacked tetrads – $(B_4)_2{\cdot}M^+$

Stacking interactions play a crucial role in stabilizing DNA structures, including quadruhelical systems.[39] All of the stacked models analyzed in this work are characterized by parallel polarity of the hydrogen bonds, which corresponds to the parallel arrangement of the strands in four-stranded nucleic acids. The final structure $(B_4)_2{\cdot}M^+$ does not include a sugar-phosphate backbone, and we are therefore able to break the formation energy down according to the individual interactions.

The formation of stacked tetrads is depicted in three steps in Figure 4. The trends observed for the base pairing and the ion coordination correlate nicely with those demonstrated for single-tetrad systems (compare Figure 3 and 4). Modifying the imidazole core (AdaX) has a rather marginal effect on the magnitude of the stacking interactions. However, substitution at position 8 of the xanthine scaffold (MX, FdaX, and CldaX) strengthens the stacking interactions. The significant modulation of the stacking observed for CldaX (8 kcal mol^{-1}) is assumed to originate in the great polarizability of the chlorine atom and the efficient redistribution of electrons when a stacked system is formed.

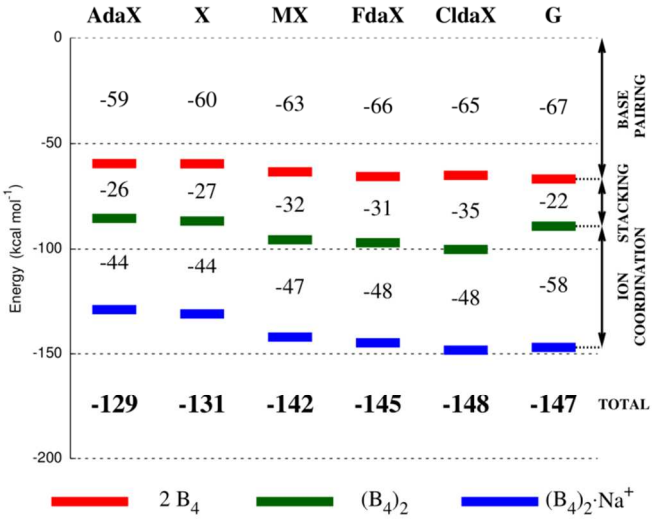

Figure 4. Contributions to the formation energy (ΔE) of the $(B_4)_2{\cdot}Na+$ system in water. The total values of the formation energy are marked in bold. The other three values represent the individual contributions of the base pairing, calculated as $\Delta E = 2 \times \{E[B_4] - 4 \times E[B]\}$; the stacking calculated as $\Delta E = E[(B_4)_2] - 2 \times E[B_4]$; and the ion coordination, calculated as $\Delta E = E[(B_4)_2 \cdot Na^+] - \{E[(B_4)_2] + E[Na^+]\}$.

The stacking energy depends on the mutual orientation (twist) of the two tetrads and their separation (rise). Different nucleobases and their derivatives exhibit different optimal values of twist that may not be fully compatible with the requirements of a sugar-phosphate backbone. To investigate this factor in detail, the stacking ability was evaluated by using two-dimensional potential energy scans employing the mutual separation (rise) and orientation (twist) of two B_4 replicas, each having C_{4h} symmetry, with an Na^+ ion incorporated in the central inter-plane position of the $(B_4)_2$. The obtained results (Figure 5; for systems containing K^+, see Figure S1) show one notably broad and shallow central minimum around 45° for $(G_4)_2{\cdot}Na^+$, which is in agreement with a very recent computational study[40] performed on a parallel arrangement of $(G_4)_2{\cdot}K^+$ in the gas phase at the MP2/6-31G*(0.25) level of theory. In contrast to the G-system, two equivalent minima (~ 30° and ~ 60°), separated by a barrier of ~3 kcal mol^{-1}, were identified for $(FdaX_4)_2{\cdot}Na^+$. The most abundant experimental value of the helical twist for parallel G-quadruplexes reportedly corresponds to a region of partly overlapping 5- and 6-membered rings (~ 60°).[40] We found such an arrangement to be the most stable for all of the xanthine derivatives, even in the absence of sugar-phosphate backbone, indicating that these systems are ideally prearranged for constructing quadruhelical nucleic acids.

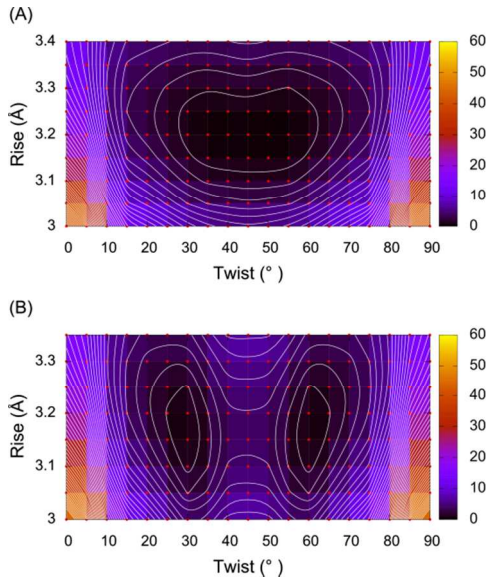

Figure 5. The impact of the twist and rise parameters on the stacking energy of the systems **A)** $(G_4)_2 \cdot Na^+$ and **B)** $(FdaX_4)_2 \cdot Na^+$. The energy contours are separated by 1 kcal mol^{-1}.

The potential use of xanthine and its derivatives as drugs would be greatly dependent upon their ability to stack properly onto guanine-based systems. Because the tetrads of guanine and xanthine exhibit different values of twist, they are not geometrically fully compatible. However, the potential energy scans show that the penalty associated with this difference in twist is rather small (ca ~3 kcal mol^{-1}) in comparison with the total stacking energy (ca ~25 kcal/mol). Thus mixed systems, such as $G_4 \cdot [FdaX]_4$ and $G_4 \cdot [CldaX]_4$ may still be sufficiently stable. The stacking energies calculated for these two mixed systems were 26 and 28 kcal mol^{-1}, respectively. These values correspond approximately to the average stacking energies determined for the $(G_4)_2$ and $(FdaX_4)_2$ and $(G_4)_2$ and $(CldaX_4)_2$ assemblies, respectively. It follows from this dependence that any modification of the xanthine core that would strengthen the stacking in a $B_4 \cdot B_4$ homo-assembly would most likely also improve the stacking in a mixed $B_4 \cdot B'_4$ system. These findings provide a tool for estimating the stability of potential ligands[9] based on the modified xanthine tetrad.

The base-cation binding is another interaction that is essential for the formation of G-based quadruplexes.[38] Our previous calculations showed that this kind of interaction is somewhat less important for X-based systems.[5,6] In this work, we have found difference in energy of approximately 10 kcal mol^{-1} for the $(B_4)_2$-ion interaction between guanine and 9-deaza-8-haloxanthine systems. However, this deficiency of the xanthine systems is balanced by the increased energy of stacking interactions. Thus the calculated total formation energies for the G (-147 kcal mol^{-1}) and FadX (-145 kcal mol^{-1}) systems are almost equal at the selected level of theory.

To check the effect of the terminate group at the position of the glycosidic bond, we compared trends in the formation energies for selected systems ending with H or CH_3 (Figure S2 in Supporting Information). Despite the different electronic properties of H and CH_3, the trends for the two systems are similar justifying the use of simple bases ending with H in this study.

Calculations employing the COSMO water model indicate only a moderate difference between the energies of Na^+ and K^+ coordination with $(B_4)_2$. The energies calculated for the binding of K^+ to $(B_4)_2$ composed of G, X, or FdaX were 2-3 kcal mol^{-1} less than those for Na^+. This contrasts with the experimental finding that G-quadruplexes preferably bind K^+ ions.[41] Detailed analysis shows that the COSMO solvent model is able to properly determinate the difference in solvation energies of the isolated ions Na^+ and K^+. The calculated difference is -17.2 kcal mol^{-1}, in good agreement with the value obtained from the experimental ion solvation energies (-16.7 kcal mol^{-1}).[42] Moreover, the solvation energies of $(B_4)_2 \cdot M^+$ are practically identical for these two ions (difference < 0.2 kcal mol^{-1}). This behavior could be expected because the cation is buried in a central pocket formed by the two tetrads and is thereby effectively screened off from the solvent. The discrepancy found between the ions is then probably related erroneous values of the energies of interaction of the ions with $(B_4)_2$ resulting from the DFT functional that was used. The COSMO solvent model is capable of describing only the polar contribution to the solvation energy. It completely neglects any non-polar contribution that might have an impact on the correct description of the formation of B_4 and $(B_4)_2$, which can expect to see a significant reorganization of the first solvent shell. These changes are reflected in increased entropy as the water molecules from the first solvation shell are released to the bulk solvent. To estimate the role of non-polar solvation contribution roughly, we employed an alternative implicit solvent model (SMD)[43] that is able to account for such effects. Although we are aware of limitations of such implicit solvent models in accounting for specific solute-solvent interactions, the results summarized in Figure S3 demonstrate that the trends in the stability of xanthine-derived systems are preserved, thereby supporting the selection of 9-deaza-8-halogen derivatives as prospective building blocks.

Formation of three stacked tetrads – $(B_4)_3 \cdot 2M^+$

Investigating stoichiometric variants of quadruplex-cation systems or the energy profile of the cation moving along the axis of the quadruplex, requires a model that includes at least three stacked tetrads. We therefore investigated selected the larger $(G_4)_3$, $(X_4)_3$, $(FdaX_4)_3$, and $(CldaX_4)_3$ systems in the absence as well as the presence of one or two identical cations (Na^+ or K^+; for data involving K^+, see Table S2). The breakdown of the formation energy shown in Figure 6 clearly demonstrates that an empty $(B_4)_3$ is characterized by a larger formation energy for X and its derivatives than for G, which indicates that the stacking interaction is a very significant stabilizing force for the X-based systems. The insertion of one or two cations between the planes of the tetrads balances the differences in the stacking energy between the G and the FdaX (or CldaX) systems, and the total formation energy calculated for the $(FdaX_4)_3 \cdot 2Na^+$ system (-256 kcal mol^{-1}) is comparable to

that for the $(G_4)_3{\cdot}2Na^+$ (-258 kcal mol^{-1}). A very similar value is also calculated for the $(CldaX_4)_3{\cdot}2Na^+$ system (-257 kcal mol^{-1}). Upon forming quadruhelical structures, these two 9-deaza-8-haloxanthine systems are expected to match the energy characteristics of natural guanine systems.

The suitability of the method used to calculate the formation energies in implicit solvent was supported by a study comparing selected xanthine derivatives using other quantum chemical methods and solvent models. Single-point RI-MP2/def2-TZVPP calculations corrected for BSSE (see Figure S4 in Supporting Information) provide the same qualitative picture of the formation energies in vacuo as the RI-BLYP-D3/def2-TZVPP method used in this work. The same qualitative picture of the formation energies in water as that calculated at the BLYP-D3/def2-TZVPP level of theory using the COSMO solvent model has also been obtained using the SMD solvent model (see Figure S5 in Supporting Information). It is noteworthy that the SMD solvent model yields significantly increased formation energies for the xanthine derivatives in comparison to guanine because of more favorable non-polar contributions.

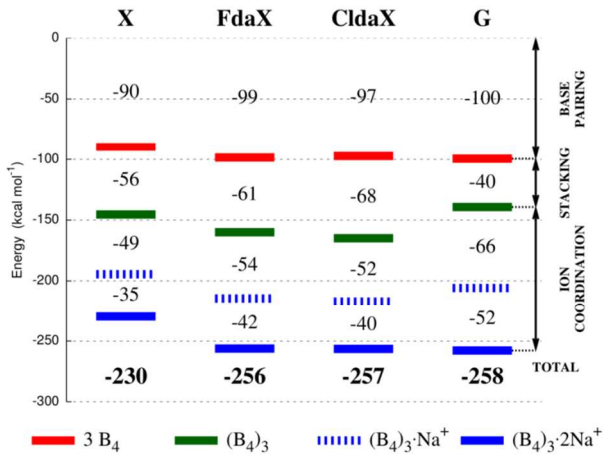

Figure 6. Contributions to the formation energy of the $(B_4)_3{\cdot}Na^+$ system in water. The total values of the formation energy are marked in bold. The other four values represent the individual contributions of the base pairing, calculated as $\Delta E = 3 \times \{E[B_4] - 4 \times E[B]\}$; the stacking, calculated as $\Delta E = E[(B_4)_3] - 3 \times E[B_4]$; the first-ion coordination, calculated as $\Delta E = E[(B_4)_3 \cdot Na^+] - \{E[(B_4)_3] + E[Na^+]\}$; and second-ion coordination, calculated as $\Delta E = E[(B_4)_3 \cdot 2Na^+] - \{E[(B_4)_3 \cdot Na^+] + E[Na^+]\}$.

Two cations are located in inter-tetrad positions between the three planes (Table S3). Its smaller radius allows Na^+ to bind closer to the terminal quartets than K^+, to minimize the mutual repulsion of cations. Thus, the binding energy related to capturing two cations in the $(B_4)_3$ system favors Na^+.

The ratio of formation energies for the binding of the second Na^+ to that of the first can be used to demonstrate the abilities of individual xanthine derivatives to partially shield the ions occupying neighboring inter-plane positions and thereby diminish the mutual repulsion of the cations. For the FdaX and CldaX derivatives, these ratios are 0.78 and 0.77, respectively, indicating that the binding of the second ion is about 22 % less favorable than that of the first. A similar value (0.79) was found for guanine. This shows that these two modified xanthine nucleobases are nearly as potent as the natural guanine reference and significantly better than unmodified xanthine (0.71).

The most suitable systems derived from xanthine are FdaX and CldaX. All of our results show that assemblies composed of these two systems exhibit the highest formation energies. We selected the FdaX derivative for further study. It has a slightly lower formation energy than CldaX but it contains fever electrons, and this enables faster QM calculations. It can also be expected that classical molecular mechanics can describe the fluorine atom more accurately than the more polarizable chlorine atom. A molecular mechanics description of the FdaX quadruplex was employed to validate the quadruplex stability using molecular dynamics.

Ion transfer in $(B_4)_3{\cdot}M^+$

The transfer of a cation was investigated in $(B_4)_3$ systems containing only a single cation. The cation was moved from one inter-plane position to the other through a pore in the central tetrad. The outer tetrads were fixed at positions derived from the geometry of a $(B_4)_3$ system containing two ions. This model (Figure S6) better describes the increased rigidity of the outer tetrads that results from their stabilization in longer quadruhelical systems. Optimization through a series of steps that allowed only the central quartet to relax at each point of the transfer of the cation, resulted in the profiles shown in Figure 7.

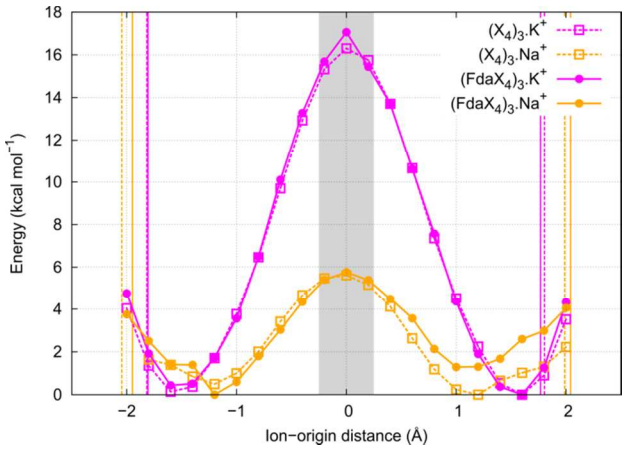

Figure 7. Energy profiles of transfer of the cations through the central tetrad of selected $(B_4)_3$ systems. The vertical lines refer to the original positions of the cations in the initial $(B_4)_3{\cdot}2M^+$ geometry, and the gray band indicates the range of positions of the central tetrad enforced during the ion transfer. For a detailed description of the model, see Supporting Information.

The barrier to the transfer of Na^+ was found to be about 6 kcal mol^{-1}, and it does not depend significantly on modification of the xanthine nucleobase. A higher barrier (about 16 kcal mol^{-1}) was found for the transfer of K^+, which is assumed to result from the larger radius of this ion. Again in this case, modification of the nucleobase was found to have only a

marginal effect. The positions of the energy minima, which identify the optimal distances of the cations from the central tetrad, also reflect the difference in the radii of the two cations. The position of the energy minimum of the sodium cation is about 1.2 Å, whereas that of the potassium cation is 1.6 Å. The opposite situation is found for the system $(B_4)_3 \cdot 2M^+$, containing two cations (depicted in Figure 7 by vertical lines). In this case the sodium cations are separated by a longer distance (d/2 = 2.0 Å) than the potassium cations (d/2 = 1.8 Å). The observed change can be explained by cation repulsion. Because of their smaller radius, the sodium ions can get closer to the outer tetrads, resulting in greater separation of the ions from each other and lower ion-ion repulsion.

In larger assemblies of $(B_4)_n \cdot (n-1)M^+$ containing more than two cations, competition between limiting situations such as the two described above can be expected. Systems containing sodium cations will deviate significantly from both of these cases because of the large difference in the position of this ion in the limiting topologies (0.8 Å). Systems containing potassium cations will probably see smaller changes because this difference is only 0.2 Å. Thus it seems that the radius of K^+ makes this ion more compatible with both of the limiting cases, which may be essential to the assembly of $(B_4)_n \cdot (n-1)M^+$.

The large difference between the positions of the ion in the limiting cases may also explain why a different mechanism for transfer of Na^+ in $d(X_4)_4$ is observed for MD simulations in explicit water solvent. The specific hydration of Na^+ with two molecules of water shifts the positions of the energy minima from an in-plane to an inter-plane arrangement (see Figure S8 in Supporting Information).[5]

The transfer of a cation is accompanied by several structural changes. Two of these, the base inclination (expressed as the distance between the center of all of the O6 atoms and the original geometrical center of the whole system) and the pore size (the average distance between opposite O6 oxygen atoms within one tetrad), are shown in Figure S7. The pore is about 0.5 Å larger for in-plane than for the inter-plane position of K^+. The modulation of the pore size is related mainly to out-of-plane distortions of the base that have amplitudes of ~ 0.2 Å (see Figure 7 and Figure S7). The transfer of Na^+ causes negligible changes in both parameters, in keeping with its smaller ionic radius.

FdaX unit in a four-stranded DNA quadruplex

To check the steric and electronic compatibility of a designed modification with the sugar-phosphate backbone in quadruhelical oligonucleotides, we incorporated one of the most promising candidates - FdaX - into a tetramolecular deoxyribonucleotide (further abbreviated as $d(FdaX_4)_4$) and examined the dynamic data provided by a Molecular Dynamics (MD) simulation. First, the initial structures contained K^+ in all three inter-plane positions. In this case the two outer potassium ions were released out of the pore during MD simulations of both the X and the FdaX systems. Second, initial structures containing K^+ in only the two outer inter-plane positions were subjected to unbiased MD simulation. The simulation of the quadruplex composed of unmodified xanthine resulted in a system containing only a single K^+ because one of ions was released during the equilibration procedure. However, the system based on FdaX and containing two potassium cations (Figure 8) remained stable during the entire 200 ns long simulation (Figure S9). The presence of two cations in $d(FdaX_4)_4$, which makes the system more rigid, can be explained by the ion-coordination energy gained by modifying xanthine. However, this stabilization does not affect the barrier to transport of the cation (Figure S8). Geometrical analysis further reveals that the C9-H fragment, which replaces the N9 atom in the xanthine structure, does not induce any steric clashes with the neighboring atoms of the deoxyribose unit (Figure 8).

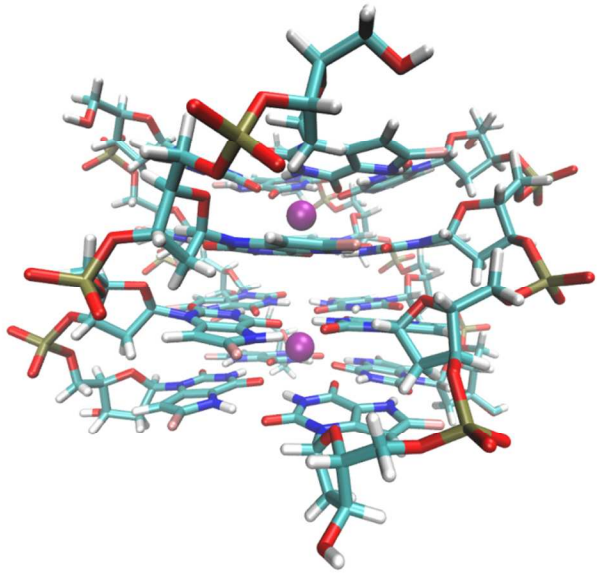

Figure 8. The average structure of $d(FdaX_4)_4$ quadruplex with two K^+ in inter-plane positions from the last 5 ns of unbiased 200 ns MD simulation.

It should be noted that position C9 allows the alternative incorporation of the FdaX block into the DNA quadruplex. This bonding is analogous to the natural glycosidic bonding of a guanine base to deoxyribose but via a C-C bond. However, the simulated quadruplex involving an FdaX unit bound to C9 exhibits greater instability than does FdaX bound to N3 and, similar to an *N3*-X system, only a single K^+ remains in a channel compartment. Generally, the overall stability of the quadruplex based on FdaX bound to C9 was somewhat lower than that involving FdaX bound to N3 but notably larger than that based on the *N3*-bonded xanthine base (Figure S10).

Conclusions

In this contribution, we report the *in silico* design of xanthine derivatives as promising candidates for constructing quadruplex-binding ligands suitable for medical applications and for the development of artificial DNA quadruplexes for bio-nanotechnology. We demonstrate that tailoring the

properties of the xanthine core can significantly enhance the base stacking and interactions with ions with almost no effect on the barrier to ion transport through the central tetrads. Our calculations indicate that 9-deaza-8-haloxanthine systems (containing fluorine or chlorine) should form more stable quadruplexes as compared to the xanthine reference, and with greater affinity for Na^+ and K^+. In addition, unbiased MD simulations show that the substitution of CH for the N9 atom in xanthine unit does not introduce any steric clashes between the artificial base and the sugar-phosphate backbone in parallel, four-stranded DNA quadruplexes.

It would be extremely interesting to see experimental data for 9-deaza-8-haloxanthine systems incorporated into quadruhelical DNA or in smart quadruplex-selective ligands. We encourage organic and biological chemists to synthesize and investigate these molecules because our work shows that the properties of 9-deaza-8-haloxanthine systems should be superior to those of xanthine and comparable to those of guanine, the natural reference. In addition, the significantly different spectroscopic properties of these artificial systems, as compared to those of the natural guanine, can be used to develop selective detection probes.[44]

Acknowledgements

This work was supported by the project "CEITEC – the Central European Institute of Technology" (CZ.1.05/1.1.00/02.0068) from the European Regional Development Fund. Access to the CERIT-SC computing and storage facilities provided under the program Center CERIT Scientific Cloud, part of the Operational Program Research and Development for Innovations, reg. no. CZ. 1.05/3.2.00/08.0144 is highly appreciated.

Notes and references

[a] CEITEC – Central European Institute of Technology, Masaryk University, Kamenice 5/A4, Brno, CZ-625 00, Czech Republic.

[b] National Center for Biomolecular Research, Faculty of Science, Masaryk University, Kamenice 5/A4, Brno, CZ-625 00, Czech Republic.

[c] Department of Chemistry, Faculty of Science, Masaryk University, Kamenice 5, Brno, CZ-625 00, Czech Republic.

* To whom correspondence should be addressed. Fax: +420-549492556, Email: rmarek@chemi.muni.cz.

† This paper is dedicated to Professor Milan Potáček on the occasion of his 70th birthday.

Electronic Supplementary Information (ESI) available: Atomic charges for the modified xanthine bases, details of the DFT calculations, formation energies, twist scans for stacking interactions in the $(B_4)_2$ system, comparison of the COSMO and SMD implicit solvent models, comparison of the MP2 and DFT-D3 formation energies, comparison of the DFT-D3 formation energies for H- and Me-terminated bases, characterization of the geometric changes during the transfer of the cation through the central tetrad in the $(B_4)_3$ system, details of the MD and ABF simulations, and RESP charges for the modified deoxyribonucleotides. DOI: 10.1039/b000000x/

1. S. Balasubramanian, L. H. Hurley, and S. Neidle, *Nat. Rev. Drug Discov.*, 2011, **10**, 261–275.
2. P. Alberti, A. Bourdoncle, B. Sacca, L. Lacroix, and J.-L. Mergny, *Org. Biomol. Chem.*, 2006, **4**, 3383–3391.
3. J. Szolomajer, G. Paragi, G. Batta, C. F. Guerra, F. M. Bickelhaupt, Z. Kele, P. Padar, Z. Kupihar, and L. Kovacs, *New J. Chem.*, 2011, **35**, 476–482.
4. C. F. Guerra, H. Zijlstra, G. Paragi, and F. M. Bickelhaupt, *Chem.- Eur. J.*, 2011, **17**, 12612–12622.
5. J. Novotny, P. Kulhanek, and R. Marek, *J. Phys. Chem. Lett.*, 2012, **3**, 1788–1792.
6. Y. P. Yurenko, J. Novotný, V. Sklenář, and R. Marek, *Phys. Chem. Chem. Phys.*, 2014, **16**, 2072–2084.
7. G. Paragi, J. Szolomájer, Z. Kupihár, G. Batta, Z. Kele, P. Pádár, B. Penke, H. Zijlstra, C. Fonseca Guerra, F. Matthias Bickelhaupt, and L. Kovács, in *Guanine Quartets*, eds. L. Spindler and W. Fritzsche, RSC Publishing, Cambridge, 2013, pp. 179–193.
8. M. Kaushik, S. Kaushik, A. Bansal, S. Saxena, and S. Kukreti, *Curr. Mol. Med.*, 2011, **11**, 744–769.
9. R. Haudecoeur, L. Stefan, F. Denat, and D. Monchaud, *J. Am. Chem. Soc.*, 2013, **135**, 550–553.
10. G. Biffi, D. Tannahill, J. McCafferty, and S. Balasubramanian, *Nat. Chem.*, 2013, **5**, 182–186.
11. G. N. Parkinson, in *Guanine Quartets*, eds. L. Spindler and W. Fritzsche, RSC Publishing, Cambridge, 2013, pp. 237–247.
12. E. Largy and M.-P. Teulade-Fichou, in *Guanine Quartets*, eds. L. Spindler and W. Fritzsche, RSC Publishing, Cambridge, 2013, pp. 248–262.
13. W. Fritzsche and L. Spindler, *Guanine quartets: structure and application*, RSC Publishing, Cambridge, 2013.
14. M. S. Kaucher, W. A. Harrell, and J. T. Davis, *J. Am. Chem. Soc.*, 2006, **128**, 38–39.
15. H. Sun, X. Li, Y. Li, L. Fan, and H.-B. Kraatz, *Analyst*, 2013, **138**, 856–862.
16. J. Davis, *Angew. Chem.-Int. Ed.*, 2004, **43**, 668–698.
17. T. Pinnavaia, C. Marshall, C. Mettler, C. Fisk, H. Miles, and E. Becker, *J. Am. Chem. Soc.*, 1978, **100**, 3625–3627.
18. M. Nikan and J. C. Sherman, *J. Org. Chem.*, 2009, **74**, 5211–5218.
19. R. Ahlrichs, M. Bar, M. Haser, H. Horn, and C. Kolmel, *Chem. Phys. Lett.*, 1989, **162**, 165–169.
20. A. Becke, *Phys. Rev. A*, 1988, **38**, 3098–3100.
21. C. Lee, W. Yang, and R. Parr, *Phys. Rev. B*, 1988, **37**, 785–789.
22. F. Weigend and R. Ahlrichs, *Phys. Chem. Chem. Phys.*, 2005, **7**, 3297–3305.
23. S. Grimme, J. Antony, S. Ehrlich, and H. Krieg, *J. Chem. Phys.*, 2010, **132**, 154104.
24. K. Eichkorn, O. Treutler, H. Ohm, M. Haser, and R. Ahlrichs, *Chem. Phys. Lett.*, 1995, **240**, 283–289.
25. F. Weigend, *Phys. Chem. Chem. Phys.*, 2006, **8**, 1057–1065.
26. A. Klamt and G. Schuurmann, *J. Chem. Soc.-Perkin Trans. 2*, 1993, 799–805.
27. M. Swart and P. T. van Duijnen, *Mol. Simul.*, 2006, **32**, 471–484.
28. M. Swart, E. Rösler, and F. M. Bickelhaupt, *Eur. J. Inorg. Chem.*, 2007, **2007**, 3646–3654.
29. S. Grimme, *J. Comput. Chem.*, 2006, **27**, 1787–1799.
30. C. Fonseca Guerra, H. Zijlstra, G. Paragi, and F. M. Bickelhaupt, *Chem. – Eur. J.*, 2011, **17**, 12612–12622.

31. T. van Mourik and A. J. Dingley, *Chem. – Eur. J.*, 2005, **11**, 6064–6079.
32. D. A. Case, T.A. Darden, T.E. Cheatham, III, C.L. Simmerling, J. Wang, R.E. Duke, R. Luo, R.C. Walker, W. Zhang, K.M. Merz, B.P. Roberts, B. Wang, S. Hayik, A. Roitberg, G. Seabra, I. Kolossváry, K.F. Wong, F. Paesani, J. Vanicek, J. Liu, X. Wu, S.R. Brozell, T. Steinbrecher, H. Gohlke, Q. Cai, X. Ye, J. Wang, M.-J. Hsieh, G. Cui, D.R. Roe, D.H. Mathews, M.G. Seetin, C. Sagui, V. Babin, T. Luchko, S. Gusarov, A. Kovalenko, and P.A. Kollman, *Amber 11*, University of California, San Francisco, 2010.
33. J. Wang, P. Cieplak, and P. Kollman, *J. Comput. Chem.*, 2000, **21**, 1049–1074.
34. A. Perez, I. Marchan, D. Svozil, J. Sponer, T. E. Cheatham, C. A. Laughton, and M. Orozco, *Biophys. J.*, 2007, **92**, 3817–3829.
35. W. L. Jorgensen, J. Chandrasekhar, J. D. Madura, R. W. Impey, and M. L. Klein, *J. Chem. Phys.*, 1983, **79**, 926–935.
36. I. S. Joung and T. E. Cheatham, *J. Phys. Chem. B*, 2008, **112**, 9020–9041.
37. U. Singh and P. Kollman, *J. Comput. Chem.*, 1984, **5**, 129–145.
38. R. D. Gray and J. B. Chaires, *Methods*, 2012, **57**, 47–55.
39. P. B. Lutz and C. A. Bayse, *Phys. Chem. Chem. Phys.*, 2013, **15**, 9397–9406.
40. C. J. Lech, B. Heddi, and A. T. Phan, *Nucleic Acids Res.*, 2013, **41**, 2034–2046.
41. N. V. Hud, F. W. Smith, F. A. L. Anet, and J. Feigon, *Biochemistry (Mosc.)*, 1996, **35**, 15383–15390.
42. Y. Marcus, *J. Chem. Soc. Faraday Trans.*, 1991, **87**, 2995–2999.
43. A. V. Marenich, C. J. Cramer, and D. G. Truhlar, *J. Phys. Chem. B*, 2009, **113**, 6378–6396.
44. M. Sproviero, K. L. Fadock, A. A. Witham, R. A. Manderville, P. Sharma, and S. D. Wetmore, *Chem. Sci.*, 2014, **5**, 788–796.

